Journal of Innovative Optical Health Sciences
Vol. 8, No. 1 (2015) 1540006 (7 pages)

DOI: 10.1142/S1793545815400064

World Scientific
www.worldscientific.com

Correlation of *in vivo* tumor response and singlet oxygen luminescence detection in mTHPC-mediated photodynamic therapy

Brian C. Wilson*,§, Michael S. Patterson†, Buhong Li‡ and Mark T. Jarvi*
*Department of Medical Biophysics
University of Toronto/University Health Network
Toronto, Ontario M5G 1L7, Canada
†Juravinski Cancer Centre and McMaster University
Hamilton, Ontario L8V 5C2, Canada
‡MOE Key Laboratory of OptoElectronic Science and Technology for Medicine
Fujian Provincial Key Laboratory for Photonics Technology
Fujian Normal University, Fuzhou, Fujian 350007, P. R. China
§wilson@uhnres.utoronto.ca

Received 28 April 2014
Accepted 12 August 2014
Published 29 September 2014

Excited-state singlet oxygen ($^1O_2$), generated during photodynamic therapy (PDT), is believed to be the primary cytotoxic agent with a number of clinically approved photosensitizers. Its relative concentration in cells or tissues can be measured directly through its near-infrared (NIR) luminescence emission, which has correlated well with *in vitro* cell and *in vivo* normal skin treatment responses. Here, its correlation with the response of tumor tissue *in vivo* is examined, using the photosensitizer meso-tetrahydroxyphenylchlorin (mTHPC) in an animal model comprising luciferase- and green fluorescent protein (GFP)-transduced gliosarcoma grown in a dorsal window chamber. The change in the bioluminescence signal, imaged pre-treatment and at 2, 5 and 9 d post treatment, was used as a quantitative measure of the tumor response, which was classified in individual tumors as "non", "moderate" and "strong" in order to reduce the variance in the data. Plotting the bioluminescence-based response vs the $^1O_2$ counts demonstrated clear correlation, indicating that $^1O_2$ luminescence provides a valid dosimetric technique for PDT in tumor tissue.

Keywords: Photodynamic therapy; singlet oxygen luminescence dosimetry; bioluminescence.

1. Introduction

The excited singlet state of oxygen ($^1O_2$), is believed to be the main cytotoxic reactive species generated during photodynamic therapy (PDT) for a number of photosensitizers used clinically (porphyrin- and chlorin-based) and for some investigational new agents.[1] The focus of the present work is on singlet oxygen dosimetry, so that it is relevant only to this class of photosensitizers and not, for example, to other compounds like palladium bacteriopheophorbides[2] (TOOKAD, WST11) that are photodynamically potent but operate through photo-induced electron transfer leading to generation of reactive oxygen species such as hydroxyl radicals.[2,3] $^1O_2$ is produced in a Type II reaction, in which the excited singlet state of the photosensitizer generated upon photon absorption by the ground-state photosensitizer molecule undergoes intersystem crossing to a long-lived triplet state. This state can then exchange energy with the triplet ground state of molecular oxygen ($^3O_2$). $^1O_2$ can decay radiatively, emitting near infrared (NIR) luminescence at around 1270 nm. However, $^1O_2$ is generally believed to have a very short lifetime (likely $\ll 1\,\mu$s) in cells and tissues,[4,5] due to its high reactivity with biomolecules, so that the luminescence signal is very weak ($\sim 1:10^8$ probability). In addition, 1270 nm is not in a favorable range for efficient photodetection using standard devices. Nevertheless, it is technically feasible using nanosecond laser pulses and an extended-wavelength photomultiplier tube (PMT) operating in time-correlated, single-photon-counting (TCSPC) mode. As reviewed by Jarvi *et al.*,[4] this so-called $^1O_2$ luminescence dosimetry (SOLD) technique is now generally accepted as the "gold standard" for PDT dosimetry and has been used as such in a number of studies, for example in characterization of novel photosensitizing agents, including activatable molecular beacons[6] and nanoparticle-based sensitizers.[7] Its validity has been demonstrated clearly in cells *in vitro*, where it has been shown to generate a "universal response curve" of cell killing vs cumulative $^1O_2$ counts generated during treatment.[8] Importantly, this response curve is independent of the individual treatment parameters such as photosensitizer concentration, light dose and oxygenation. Its validity has also been demonstrated in normal skin models[9,10] and in normal human skin using a time-integrated technique,[11,12] although the latter may have limitations due to interference from background tissue and photosensitizer fluorescence and/or phosphorescence. SOLD has been demonstrated in a brain tumor model *in vivo* by Yamamoto *et al.*,[13] but without applying spectral scanning to remove background signals. Recently, Schlothauer *et al.*[14] investigated the $^1O_2$ luminescence generated from topically applied photosensitizer in pig ear skin *in vitro*, and the data showed that the $^1O_2$ kinetics coincides with the microarchitecture of epidermis, such as in fissures and hair follicles. In order to predict the clinical phototoxic response (erythema) resulting from PDT with aminolevulinic acid-induced protoporphyrin IX, Mallidi *et al.*[12] compared discrete photosensitizer fluorescence-based metrics with corresponding $^1O_2$ luminescence-based metrics. They suggested that, at least for this photosensitizer, a dose metric based on its fluorescence photobleaching may be adequate to predict the PDT outcome. While this technique is more clinically applicable at present than SOLD, Jarvi *et al.*[15] have shown that it may not work for all photosensitizers, depending on parameters such as the level of oxygenation.

Given that there are a number of both technical and conceptual reasons why measuring the volume-averaged $^1O_2$ concentration may fail in the complex and heterogeneous milieu of solid tumors,[16] the objective of this study was to test, in a well-controlled tumor model *in vivo* and using the most robust spectrally resolved TCSPC technique, whether SOLD does correlate with tumor response. Importantly, to our knowledge this is the first study showing correlation of *in vivo* tumor response with the $^1O_2$ generated during treatment using a SOLD technique that incorporates both spectral discrimination and time-resolved single photon counting to ensure that the NIR photons detected are from $^1O_2$ decay only and are not potentially confounded by unknown background contributions.

2. Materials and Methods

2.1. *Animal model*

The well-established dorsal skin-fold window chamber tumor model was used, as shown in Fig. 1(a). Briefly, window chambers were implanted on female NCRNu mice (22–28 g) anesthetized by intraperitoneal (*i.p.*) injection of Xylazine (10 mg/kg) and Ketamine (80 mg/kg). For this a 10 mm diameter circular incision was made and the skin from one

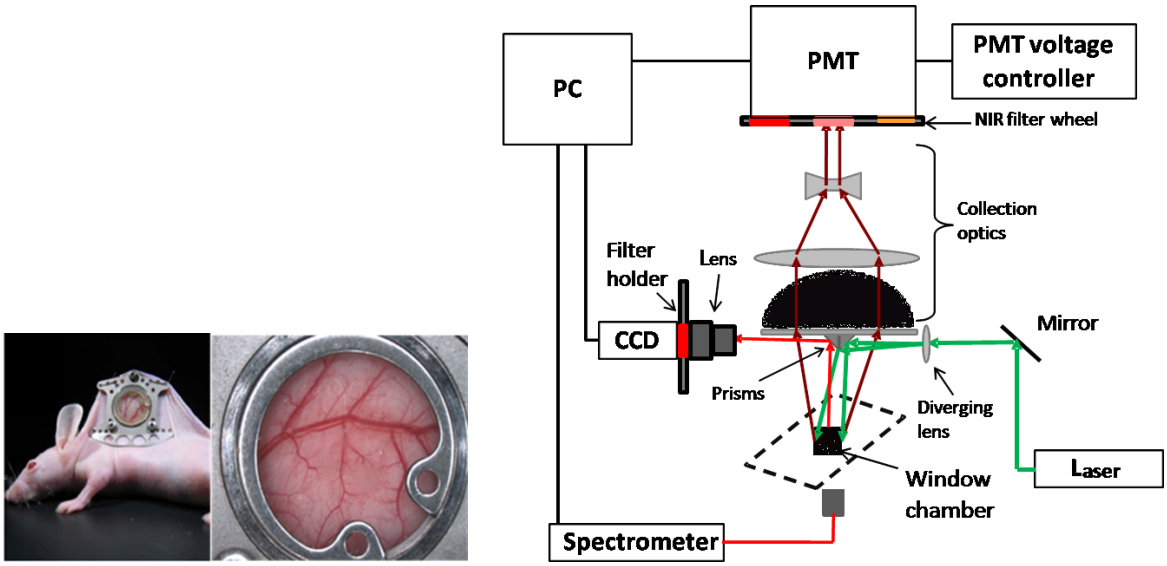

(a) (b)

Fig. 1. Experimental setup. (a) Window chamber model shown in place on the imaging stage. (b) SOLD system: PMT, photomultiplier tube; CCD, intensified charge coupled device camera for fluorescence imaging; PC, personal computer. Note that the data from the fluorescence spectrometer are not included in the present analysis.

side of the dorsal skin fold was removed. A titanium chamber was fastened with three screws at the site of incision. A circular glass coverslip was positioned over the opening and clamped to the chamber with a retaining ring. These chambers typically remain viable for several weeks, with the animal housed under normal conditions. 9L gliosarcoma tumor cells were transduced via lentivirus vectors to express both green fluorescent protein (GFP) and luciferase (luc) and a highly expressing clone was selected based on the GFP fluorescence signal and the luciferase-mediated bioluminescence signal. These transduced cells, $9L^{luc-GFP}$, were passaged in Dulbecco's modified medium supplemented with 10% fetal bovine serum and grown to confluence at 37°C under 5% CO_2. Cells were removed with trypsin, centrifuged and re-suspended in fresh media at a density of 1.5×10^7 cells/mL for implantation on the same day the chambers were installed. The coverslip was temporarily removed and 8 μL of tumor cell suspension was injected into the fascia of the subcutaneous skin layer opposite the window. The injection site was standardized to the upper center of the chamber near to a large vessel.

2.2. *PDT treatment*

The mice were treated 7–8 days after tumor implantation. About 4 h prior to light delivery, meso-tetrahydroxyphenylchlorin (mTHPC: Biolitec, Vienna, Austria) in clinical formulation and dilution 1:20 in 40% ethanol and 60% polypropylene glycol was injected *i.p.* Although it has a number of limitations, mTHPC was selected as a model photosensitizer here, since it is clinically approved (in Europe for treatment of head and neck cancers) and has been used in previous $^1O_2$ dosimetry studies.[15] About 4 h later, mice were re-anesthetized and restrained on a heated stage. Each mouse received a fixed radiant exposure of 12 J cm^{-2} at an irradiance of either 35 or 100 mW cm^{-2} from a 523 nm diode laser over a 5 mm diameter spot centered on the tumor, as visualized by the GFP fluorescence. The treatment and control cohorts were: 35 mW cm^{-2} and 0.6 mg/kg mTHPC ($n = 12$); 100 mW cm^{-2} and 0.6 mg/kg mTHPC ($n = 9$); 35 mW cm^{-2} light-only controls ($n = 3$) and 100 mW cm^{-2} light-only controls ($n = 3$). After treatment, the mice were recovered and returned to normal housing under subdued lighting.

2.3. *SOLD and fluorescence imaging/spectroscopy*

NIR luminescence was detected using the system shown in Fig. 1(b), the basis of which has been described in detail previously.[4,8] Briefly, a frequency-doubled Nd:YLF laser (QG-523–500; CrystaLaser

Inc., Reno, NV, USA) generated ~ 10 ns pulses of 523 nm light at a pulse repetition rate of ~ 10 kHz and average power of < 200 mW. This was expanded by a lens to a uniform (top hat) 5 mm diameter spot at the window chamber. The light collected from the tumor passed through a 5-position filter wheel that sampled the NIR luminescence spectrum at 1212, 1240, 1272, 1304 and 1332 nm (20 nm FWHM) before being passed to a PMT with extended NIR sensitivity (R5509-14: Hamamatsu Corp., Bridgewater, NJ, USA). The PMT was connected to a TCSPC system triggered by the laser pulse. A small silver-coated prism on the detection optical axis reflected part of light through 600 nm long-pass and 650 ± 50 nm bandpass filters to an intensified CCD camera for simultaneous imaging of the white light and GFP fluorescence.

2.4. *Bioluminescence imaging*

Bioluminescence images (BLI) and tumor-cell GFP fluorescence images were collected under general anesthesia to evaluate the tumor response to treatment. In the present analysis, the GFP imaging was used simply as a cross check that the BLI properly reported the viable tumor. At 1 week following tumor implantation the mice were injected with 100 μL (150 mg/kg) of D-luciferin dissolved in freshly prepared phosphate buffered saline. The mice (typically 5 at a time) were then placed in a whole-body imaging system (IVIS: Perkin Elmer, Waltham, MA, USA). Starting at 2 min post injection, BLI were acquired every 1 min up to 20 min and then every 2 min up to 34 min to track the kinetics of the bioluminescence signal. In addition, a GFP image ($\lambda_{ex} = 445$–490 nm, $\lambda_{em} = 515$–575 nm) was acquired at the 2.5, 7.5, 20 and 33 min time points. This imaging procedure was performed 5 times for each cohort of mice: 48 h pre-treatment; 4 h pre-treatment, immediately before photosensitizer injection; 2, 5 and 9 d post treatment. Additionally, one cohort ($n = 5$) was imaged daily for the first 8 d post tumor implantation to evaluate the tumor growth kinetics. In each animal, the ratio, $R = C_{post}/C_{pre}$, was calculated, where C_{pre} represents the total BLI counts over the tumor immediately before PDT and C_{post} represents the total counts at a specific time point following treatment. At each post-treatment time point, this ratio was then averaged over all animals.

3. Results

Response to PDT treatment was based on the changes in the BLI counts integrated over the whole tumor. The average ratios for each post-treatment time point were then classified into "no response" ($R > 1$: continued tumor growth), "moderate response" ($R = 0.5$–1: tumor stasis or slight reduction) or "strong response" ($R < 0.5$: at least 2-fold reduction in viable tumor cells). Such non-parametric classification of PDT response has been reported by Ascencio *et al.*[17] and was applied here in order to address the high tumor-to-tumor variability seen both in the BLI images and SOLD counts, and Fig. 2 presents examples of each response, at a particular time (5 d) post-treatment. For the "strong response" case, there is little remaining bioluminescence signal after treatment. Conversely, in the "no response" tumors the BLI images before and after treatment showed little change, similar to the light-only controls. We note that the fact that the BLI showed little change in the control (light-only) animals at 5 d post treatment suggests that the tumor may have reached its growth limit by the time of treatment, i.e., at 7–8 days following implantation: this is not unexpected in the chamber model where the tumor is physically confined on one side by the window and on the opposite side by the overlying skin.

Quantitative bioluminescence imaging has also been used in previous studies of PDT treatment response[18] and was further validated here [Fig. 3(a)]

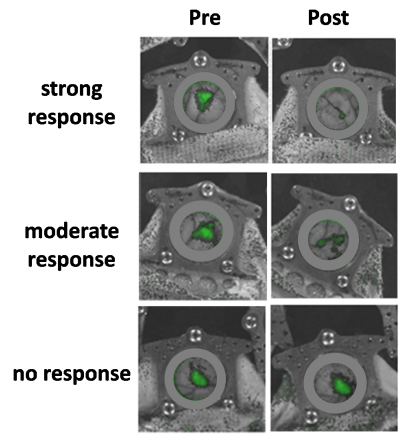

Fig. 2. Representative BLI for the different levels of treatment response at 5 d post treatment. The green signal is the false-color intensity of the BLI signal. The ring in the gray-scale photograph in each case delineates the transparent window within which the bioluminescence (and fluorescence) images are collected.

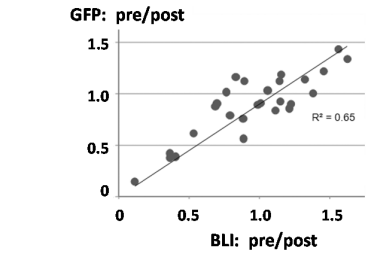

(a)

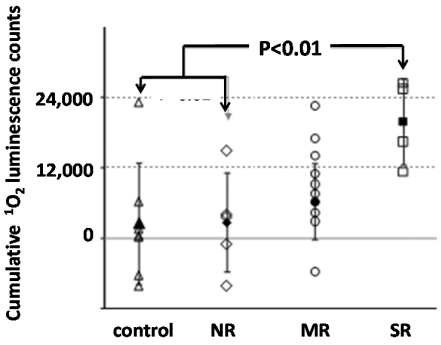

(b)

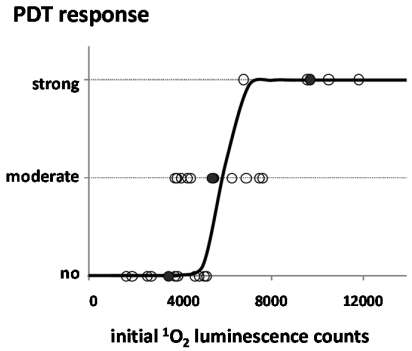

(c)

Fig. 3. (a) Correlation between GFP and bioluminescence imaging, plotting in each case the ratio of the integrated image signal before and at 5 d after PDT treatment: each point corresponds to an individual tumor. (b) Cumulative luminescence counts in individual tumors (open symbols) and averaged over all tumors (solid symbols) for each of the BLI treatment response groups. Note that the negative data points are the results of noise in the background subtraction at low $^1O_2$ signal levels. (c) Sigmoidal BLI response plot, using the initial $^1O_2$ luminescence counts at the start of PDT treatment as the dose metric, which is an alternative to the cumulative SOLD counts used in (a).

by comparison with the observed changes in the GFP signal that also reports functionally active tumor cells. Figures 3(b) and 3(c) then summarize the treatment response results, plotted in two different ways. Figure 3(b) shows how the cumulative $^1O_2$ luminescence counts in individual animals, as well as the averages over all animals, differs between the response groups. Despite the high level of scatter in the data, which is presumably related to the variability in mTHPC uptake and tissue oxygenation in the heterogeneous tumors, there is a clear trend to higher $^1O_2$ levels in those tumors showing the greatest level of cell kill: this was statistically significant (Student's t-test) between the "strong-response" group and both the "control" and "no response" groups. Plotting the data as a more conventional response curve in Fig. 3(c) shows again the high scatter between tumors, but there is a clear response–dose relationship consistent with a sigmoidal response, as might be expected.

4. Discussion and Conclusions

This study has demonstrated the validity of $^1O_2$ luminescence as a valid PDT dose metric in an *in vivo* tumor model. This extends work in photosensitizer solution, tumor cells *in vitro* and normal tissue (skin) *in vivo*, reported previously by ourselves[8,9] and by other groups[10–12,14] using variations on the SOLD instrumentation, measurement technique and biological models. The most direct comparison can be made with the *in vivo* study by Yamamoto *et al.*,[13] in which $^1O_2$ luminescence dosimetry was used in a gliosarcoma tumor xenograft model, assessing the PDT response by quantitative histopathology. They showed that, for a given total light fluence, both the $^1O_2$ counts and the tumor response decreased as the fluence rate increased (from 30 to 120 mWcm^{-1} using an interstitial diffusing fiber to deliver the light). This reduction in PDT efficacy at high light fluence rates has been reported also *in vitro*[19] and *in vivo*[20] and is well understood in terms of photochemical depletion of ground-state molecular oxygen.[21] A particular advantage of the luminescence instrument used by Yamamoto *et al.*[13] was the ability to collect the luminescence emitted from the tumor by a fiber optic bundle. However, the signal was neither spectrally resolved nor time-gated to remove the prompt NIR signal ($<\sim 1\,\mu$s after the excitation pulse) so that, as discussed by Jarvi *et al.*[15] and Lin *et al.*,[22] there may be significant contributions from background fluorescence and/or phosphorescence. Hence, we believe that the present work represents the first demonstration of the correlation between

in vivo tumor response and $^1O_2$ using a rigorously validated SOLD system.

We note that, as discussed elsewhere,[23] measurements done at the same time in these experiments using speckle-variance optical coherence tomography to image changes in the tumor microvasculature also demonstrated good correlation with $^1O_2$ generation. Hence, there is reason to believe that volume-averaged $^1O_2$ dosimetry is a valid metric for vascular as well as cellular responses, at least using this particular photosensitizer.

These results also confirm the value of SOLD as a gold standard comparator for indirect methods, such as the use of secondary fluorescent reporter molecules[24] whose spectral characteristics change upon chemical interaction with $^1O_2$. They also motivate the development of new technologies for this purpose, including NIR-sensitive imaging arrays[25] and superconducting nanowire photodetectors that have much higher 1270 nm quantum efficiency than the best PMTs and that have recently been demonstrated for $^1O_2$ luminescence detection through single optical fibers.[26] Both advances should facilitate the translation of SOLD into clinical applications, where a robust method for monitoring the true administered PDT "dose" in patients currently impedes the adoption of this modality. This is particularly true in oncology, where the tumor responses can be highly variable even for the same applied photosensitizer and light doses.[1,27]

One of the limitations of the present study was that the use of the window chamber, which has the advantage of providing direct and quantitative assessment of the tumor response to PDT, meant that it was not possible to determine if the long-term treatment response also correlates well with the SOLD measurement, since the chamber preparation only remains viable for a few weeks. Clearly, this is of the greatest interest for potential clinical applications. Hence, in the next phase of this work one promising option is to use the aforementioned fiber-coupled nanowire detectors[25] for interstitial SOLD measurements so that a subcutaneous or even an orthotopic tumor model can be used in order to follow the responses over a much longer period.

Acknowledgments

This work was supported by the Canadian Cancer Society Research Institute (014245) and the Fujian Provincial Natural Science Foundation (2011J06022). The authors wish to thank Dr. Jeffrey Medin for preparing the luc-GFP transduced cells. mTHPC was kindly supplied by Biolitec AG, Austria.

References

1. P. Agostinis, K. Berg, K. A. Cengel, T. H. Foster, A. W. Girotti, S. O. Gollnick, S. M. Hahn, M. R. Hamblin, A. Juzeniene, D. Kessel, M. Korbelik, J. Moan, P. Mroz, D. Nowis, J. Piette, B. C. Wilson and J. Golab, "Photodynamic therapy of cancer: An update," *CA Cancer J. Clin.* **61**, 250–281 (2011).
2. I. Ashur, R. Goldschmidt, I. Pinkas, Y. Salomon, G. Szewczyk, T. Sarna, A. Scherz, "Photocatalytic generation of oxygen radicals by the water-soluble bacteriochlorophyll derivative WST11, noncovalently bound to serum albumin," *J. Phys. Chem. A* **16**, 8027–8037 (2009).
3. D. Kessell, J. Reiners Jr., "Light-activated pharmaceuticals: Mechanisms and detection," *Isr J. Chem.* **52**, 674–680 (2012).
4. M. T. Jarvi, M. J. Niedre, B. C. Wilson, "Singlet oxygen luminescence dosimetry (SOLD) for photodynamic therapy: Current status and future prospects," *Photochem. Photobiol.* **82**, 1198–1210 (2006).
5. S. Hackbarth, J. Schlothauer, A. Preuss, B. Röder, "New insights to primary photodynamic effects–Singlet oxygen kinetics in living cells," *J. Photochem. Photobiol. B* **98**, 173–179 (2010).
6. G. Zheng, J. Chen, K. Stefflova, M. T. Jarvi, B. C. Wilson, "Photodynamic molecular beacon as an activatable photosensitizer based on protease controlled singlet oxygen quenching and activation," *Proc. Natl. Acad. Sci. (USA)* **104**, 8989–8994 (2007).
7. C. Yu, T. Canteenwala, M. E. El-ourly, Y. Akari, K. Pritzker, O. Ito, B. C. Wilson, L. Y. Chiang, "Efficiency of singlet oxygen production from self-assembled nanospheres of molecular micelle-like photosensitizers FC_4S," *J. Med. Chem.* **15**, 1857–1864 (2005).
8. M. J. Niedre, A. J. Secord, M. S. Patterson, B. C. Wilson, "*In Vitro* tests of the validity of singlet oxygen luminescence measurements as a dose metric in photodynamic therapy," *Cancer Res.* **53**, 7986–7994 (2003).
9. M. J. Niedre, C. S. Yu, M. S. Patterson, B. C. Wilson, "Singlet oxygen luminescence as an *in vivo* photodynamic therapy dose metric: Validation in normal mouse skin with topical aminolevulinic acid," *Br. J. Cancer* **92**, 298–304 (2005).
10. J. C. Schlothauer, S. Hackbarth, L. Jäger, K. Drobniewski, H. Patel, S. M. Goran, B. Röder, "Time-resolved singlet oxygen luminescence detection under

photodynamic therapy relevant conditions: Comparison of *ex vivo* application of two photosensitizer formulations," *J. Biomed. Opt.* **17**, 115005 (2012).

11. S. Lee, L. Zhu, A. M. Minhaj, M. F. Hinds, D. H. Vu, D. I. Rosen, S. J. Davis, T. Hasan, "Pulsed diode laser-based monitor for singlet molecular oxygen," *J. Biomed. Opt.* **13**, 034010 (2008).
12. S. Mallidi, S. Anbil, S. Lee, D. Manstein, S. Elrington, G. Kositratna, D. Schoenfeld, B. Pogue, S. J. Davis, T. Hasan, "Photosensitizer fluorescence and singlet oxygen luminescence as dosimetric predictors of topical 5-aminolevulinic acid photodynamic therapy induced clinical erythema," *J. Biomed. Opt.* **19**, 028001 (2014).
13. J. Yamamoto, S. Yamamoto, T. Hirano, S. Li, M. Koide, E. Kohno, M. Okada, C. Inenaga, T. Tokuyama, N. Yokota, S. Terakawa, H. Namba, "Monitoring of singlet oxygen is useful for predicting the photodynamic effects in the treatment for experimental glioma," *Clin. Cancer Res.* **12**, 7132–7139 (2006).
14. J. C. Schlothauer, J. Falckenhayn, T. Perna, S. Hackbarth, B. Röder, "Luminescence investigation of photosensitizer distribution in skin: Correlation of singlet oxygen kinetics with the microarchitecture of the epidermis," *J. Biomed. Opt.* **18**, 115001 (2013).
15. M. T. Jarvi, M. J. Niedre, M. S. Patterson, B. C. Wilson, "The influence of oxygen depletion and photosensitizer triplet-state dynamics during photodynamic therapy on accurate singlet oxygen luminescence monitoring and analysis of treatment dose response," *Photochem. Photobiol.* **87**, 223–234 (2011).
16. K. K. Wang, S. Mitra, T. H. Foster, "Photodynamic dose does not correlate with long-term tumor response to mTHPC-PDT performed at several drug-light intervals," *Med. Phys.* **35**, 3518–3526 (2008).
17. M. Ascencio, P. Collinet, M. O. Farine, S. Mordon, "Protoporphyrin IX fluorescence photobleaching is a useful tool to predict the response of rat ovarian cancer following hexaminolevulinate photodynamic therapy," *Lasers Surg. Med.* **40**, 322–341 (2008).
18. E. Moriyama, S. K. Bisland, L. Lilge, B. C. Wilson, "Bioluminescence imaging of the response of rat gliosarcoma to ALA-PpIX-mediated photodynamic therapy," *Photochem. Photobiol.* **80**, 241–249 (2004).
19. S. Coutier, S. Mitra, L. N. Bezdetnaya, R. M. Parache, I. Georgakoudi, T. H. Foster, F. Guillemin, "Effects of fluence rate on cell survival and photobleaching in meta-tetra-(hydroxyphenyl) chlorine photosensitized Colo 26 multicell tumor spheroids," *Photochem. Photobiol.* **73**, 297–303 (2001).
20. D. J. Robinson, H. S. de Bruijn, N. van der Veen, M. R. Stringer, S. B. Brown, W. M. Star, "Fluorescence photobleaching of ALA-induced protoporphyrin IX during photodynamic therapy of normal hairless mouse skin: The effect of light dose and irradiance and the resulting biological effect," *Photochem. Photobiol.* **67**, 140–149 (1998).
21. T. H. Foster, R. S. Murant, R. G. Bryant, R. S. Knox, S. L. Gibson, R. Hilf, "Oxygen consumption and diffusion effects in photodynamic therapy," *Radiat. Res.* **126**, 296–303 (1991).
22. H. Lin, D. Chen, M. Wang, J. Lin, S. Xie, B. Li, "Influence of pulse height discrimination threshold for photon counting on the accuracy of singlet oxygen luminescence measurement," *J. Opt.* **13**, 125301 (2011).
23. A. Mariampillai, "Development of a high resolution microvascular imaging toolkit for optical coherence tomography," PhD Thesis, University of Toronto, Canada (2010).
24. H. Lin, Y. Shen, D. Chen, L. Lin, B. C. Wilson, B. Li, S. Xie, "Feasibility study on quantitative measurements of singlet oxygen generation using singlet oxygen sensor green," *J. Fluoresc.* **23**, 41–47 (2013).
25. L. Lin, H. Lin, D. Chen, L. Chen, M. Wang, S. Xie, Y. Gu, B. C. Wilson, B. Li, "Direct imaging of singlet oxygen luminescence generated in blood vessels during photodynamic therapy," *Proc. SPIE* **9129**, 912920 (2014).
26. N. R. Gemmell, A. McCarthy, B. Liu, M. G. Tanner, S. D. Dorenbos, V. Zwiller, M. S. Patterson, G. S. Buller, B. C. Wilson, R. H. Hadfield, "Singlet oxygen detection with fibre-coupled superconducting nanowire single photon detectors," *Opt. Express* **21**, 5005–5013 (2013).
27. J. Trachtenberg, R. A. Weersink, S. R. Davidson, M. A. Haider, A. Bogaards, M. R. Gertner, A. Evans, A. Scherz, J. Savard, J. L. Chin, B. C. Wilson, M. Elhilali, "Vascular-targeted photodynamic therapy (padoporfin, WST09) for recurrent prostate cancer after failure of external beam radiotherapy: A study of escalating light doses," *BJU Int.* **102**, 556–562 (2008).